

3. Stopping Power and Range for Nuclei

Stopping power and range values can be deduced for any ion in a non-crystalline material based on semi-empirical proton stopping power values. The theory of ion-solid interactions is well established, but too complete to present here. It has been discussed in detail, e.g., by Ziegler, Biersack, and Littmark¹, where the authors also describe the computer program TRIM² which can be used for calculating stopping power and range for ion/target combinations with $Z \leq 92$.

Nuclear Stopping: The total stopping power S_t , is the sum of the electronic stopping power, S_e , due to interactions with target electrons, and the nuclear stopping power, S_n , due to interactions with target nuclei.

$$S_t = S_e + S_n . \quad (1)$$

For sufficiently high projectile energies, $S_t \approx S_e$.

S_n , in units of $\text{eV}/(10^{15} \text{ atoms/cm}^2)$, for any projectile with energy E (kev), is given by

$$S_n(E) = \frac{8.462Z_1Z_2M_1S_n(\epsilon)}{(M_1 + M_2)(Z_1^{0.23} + Z_2^{0.23})} , \quad (2)$$

where the reduced ion energy, ϵ , is defined as

$$\epsilon = \frac{32.53M_1M_2(E/M_1)}{Z_1Z_2(M_1 + M_2)(Z_1^{0.23} + Z_2^{0.23})} , \quad (3)$$

M_1 and M_2 are the projectile and target masses (amu), and Z_1 and Z_2 are the projectile and target atomic numbers. For $\epsilon \leq 30$ keV,

$$S_n(\epsilon) = \frac{\ln(1 + 1.1383\epsilon)}{2(\epsilon + 0.01321\epsilon^{0.21226} + 0.19593\epsilon^{0.5})} . \quad (4)$$

For $\epsilon > 30$ keV, unscreened nuclear stopping is used, and $S_n(\epsilon)$ simplifies to

$$S_n(\epsilon) = \frac{\ln\epsilon}{2\epsilon} . \quad (5)$$

S can be converted to units of $\text{MeV}/(\text{mg/cm}^2)$ by multiplying by $0.6022/M_2$.

Experimental proton stopping power data are summarized by Anderson and Ziegler³. Reliable data are available for many elements over a wide range of energies. However, in order to obtain values for all elements over a continuous range of proton energies, the authors fit curves through the available experimental data to generate coefficients for use in a semi-empirical parameterization of the stopping power as a function of proton energy E (keV) and the target atomic number Z_2 . S_e is assumed to be proportional to $E^{0.45}$ for $E < 25$ keV, except for $Z_2 \leq 6$, where it is proportional to $E^{0.25}$; for $25 \text{ keV} \leq E \leq 10 \text{ MeV}$, Ziegler *et al.* use

$$\frac{1}{S_e} = \frac{1}{S_{LOW}} + \frac{1}{S_{HIGH}} \quad (6)$$

where, for protons of energy E (keV),

$$S_{LOW} = A_1E^{A_2} + A_3E^{A_4} \quad (7)$$

and

$$S_{HIGH} = \frac{A_5\ln(\frac{A_6}{E} + A_7E)}{E^{A_8}} , \quad (8)$$

and the coefficients A_i for each Z_2 , available from TRIM² (which supersedes reference 1), are shown in Table 1. For $10 \text{ MeV} \leq E \leq 2 \text{ GeV}$, TRIM² includes four additional coefficients A_9 through A_{12} , shown in Table 2, for use in the parameterization

$$S_e = A_9 + A_{10}\left(\frac{\ln E}{E}\right) + A_{11}\left(\frac{\ln E}{E}\right)^2 + A_{12}\left(\frac{E}{\ln E}\right) . \quad (9)$$

¹ J.F. Ziegler, J.P. Biersack, and U. Littmark, *The Stopping and Range of Ions in Solids*, Vol. 1 of "The Stopping and Ranges of Ions in Matter", Pergamon Press, New York (1985).

² TRIM version 92.16, J.F. Ziegler and J.P. Biersack; updated version of a computer code for calculating stopping and ranges, described in reference 1.

³ H.H. Andersen and J.F. Ziegler, *Hydrogen Stopping Powers and Ranges in All Elements*, Vol. 2 of "The Stopping and Ranges of Ions in Matter", Pergamon Press, New York (1977).

Table 1. Coefficients for low-energy proton electronic stopping power parameterization.

Z_2	v_F	A_1	A_2	A_3	A_4	A_5	A_6	A_7	A_8
1	1.00000	0.01217	0.0053358	1.12874	0.36420	1120.70	1.12128	2477.31	0.009771
2	1.00000	0.48900	0.0050512	0.86135	0.46741	745.38	1.04227	7988.39	0.033329
3	0.59782	0.85837	0.0050147	1.60445	0.38844	1337.30	1.04703	2659.23	0.018980
4	1.07810	0.87810	0.0051049	5.42316	0.20320	1200.62	1.02111	1401.84	0.038529
5	1.04860	1.46080	0.0048836	2.33802	0.44249	1801.27	1.03522	1784.12	0.020240
6	1.00000	2.10544	0.0049079	2.08723	0.46258	1779.22	1.01472	2324.45	0.020269
7	1.00000	0.64564	0.0050829	4.09503	0.33879	2938.49	1.04017	2911.08	0.010722
8	1.00000	0.75109	0.0050300	3.93983	0.34620	2287.85	1.01171	3997.24	0.018427
9	1.00000	1.30187	0.0051414	3.82737	0.28151	2829.94	1.02762	7831.30	0.020940
10	1.00000	4.73391	0.0044506	0.02986	1.49404	1825.36	0.97896	130.76	0.021577
11	1.00000	6.09725	0.0044292	3.19294	0.45763	1363.35	0.95182	2380.61	0.081835
12	0.71074	14.01311	0.0043646	2.26412	0.36326	2187.37	0.99098	6264.80	0.046200
13	0.90519	0.03909	0.0045417	6.96924	0.32976	1688.30	0.95944	1151.98	0.048982
14	0.97411	2.17813	0.0044455	2.60452	0.60885	1550.21	0.93302	1703.85	0.031620
15	0.97184	17.57548	0.0038346	0.07869	1.23881	2805.97	0.97284	1037.59	0.012879
16	1.00000	3.14730	0.0044716	4.97470	0.41024	4005.80	1.00110	1898.80	0.007659
17	1.00000	3.35440	0.0044740	5.92060	0.41003	4403.90	0.99623	2006.90	0.008231
18	1.00000	2.03789	0.0044775	3.07429	0.54773	3505.01	0.97575	1714.05	0.011701
19	0.36552	0.74171	0.0043051	1.15147	0.95083	917.21	0.87820	389.93	0.189258
20	0.62712	9.13157	0.0043809	5.46107	0.31327	3891.81	0.97933	6267.93	0.015196
21	0.81707	7.22475	0.0043718	6.10169	0.37511	2829.22	0.95218	6376.12	0.020398
22	0.99430	0.14700	0.0048456	6.34846	0.41057	2164.13	0.94028	5292.62	0.050263
23	1.14230	5.06114	0.0039867	2.61740	0.57957	2218.88	0.92361	6323.03	0.025669
24	1.23810	0.53267	0.0042968	0.39005	1.27254	1872.68	0.90776	64.17	0.030107
25	1.12220	0.47697	0.0043038	0.31451	1.32893	1920.54	0.90649	45.58	0.027469
26	0.92705	0.02743	0.0035443	0.03156	2.17547	1919.55	0.90099	23.90	0.025363
27	1.00470	0.16383	0.0043042	0.07345	1.85917	1918.42	0.89678	27.61	0.023184
28	1.20000	4.25623	0.0043737	1.56057	0.72067	1546.84	0.87958	302.02	0.040944
29	1.06610	2.35083	0.0043237	2.88205	0.50113	1837.72	0.89992	2376.95	0.049650
30	0.97411	3.10952	0.0038455	0.11477	1.50371	2184.69	0.89309	67.31	0.016588
31	0.84912	15.32177	0.0040306	0.65391	0.67668	3001.71	0.92484	3344.18	0.016366
32	0.95000	3.69319	0.0044813	8.60801	0.27638	2982.66	0.92760	3166.57	0.030874
33	1.09030	7.13728	0.0043134	9.42470	0.27937	2725.83	0.91597	3166.08	0.025008
34	1.04290	4.89794	0.0042937	3.77931	0.50004	2824.50	0.91028	1282.42	0.017061
35	0.49715	1.36827	0.0043024	2.56787	0.60822	6907.83	0.98170	628.01	0.006805
36	0.37755	2.23528	0.0043096	4.88562	0.47883	4972.28	0.95146	1185.23	0.009236
37	0.35211	0.42056	0.0041169	0.01695	2.36159	2252.73	0.89192	39.75	0.027757
38	0.57801	30.77977	0.0037736	0.55813	0.76816	7113.16	0.97697	1604.39	0.006527
39	0.77773	11.57598	0.0042119	7.02444	0.37764	4713.52	0.94264	2493.22	0.011270
40	1.02070	6.24058	0.0041916	5.27012	0.49453	4234.55	0.93232	2063.92	0.011844
41	1.02900	0.33073	0.0041243	1.72460	1.10621	1930.19	0.86907	27.42	0.038208
42	1.25420	0.01775	0.0041715	0.14586	1.73052	1803.62	0.86315	29.67	0.032123
43	1.12200	3.72287	0.0041768	4.62860	0.56769	1678.02	0.86202	3093.95	0.062440
44	1.12410	0.13998	0.0041329	0.25573	1.42411	1919.26	0.86326	72.80	0.032235
45	1.08820	0.28590	0.0041386	0.31301	1.34235	1954.82	0.86175	115.18	0.029342
46	1.27090	0.76002	0.0042179	3.38597	0.76285	1867.39	0.85805	69.99	0.036448
47	1.25420	6.39568	0.0041935	5.46891	0.41378	1712.61	0.85397	18493.00	0.056471
48	0.90094	3.47169	0.0041344	3.23372	0.63788	1116.36	0.81959	4766.03	0.117895
49	0.74093	2.52651	0.0042282	4.53198	0.53562	1030.85	0.81652	16252.23	0.197218
50	0.86054	7.36830	0.0041007	4.67911	0.51428	1160.00	0.82454	17964.82	0.133160
51	0.93155	7.71972	0.0043880	3.24198	0.68434	1428.11	0.83398	1786.67	0.066512
52	1.00470	16.77990	0.0041918	9.31977	0.29568	3370.92	0.90289	7431.72	0.026160
53	0.55379	4.21323	0.0042098	4.67533	0.57945	3503.93	0.89261	1468.87	0.014359
54	0.43289	4.61889	0.0042203	5.81644	0.52184	3961.24	0.90410	1473.26	0.014195
55	0.32636	0.18517	0.0036215	0.00059	3.53154	2931.30	0.88936	26.18	0.026393
56	0.51310	4.82483	0.0041458	6.09343	0.57026	2300.11	0.86359	2980.72	0.038679
57	0.69500	0.49857	0.0041054	1.97754	0.95877	786.55	0.78509	806.60	0.408824
58	0.72591	3.27544	0.0042177	5.76803	0.54054	6631.29	0.94282	744.07	0.008303
59	0.71202	2.99783	0.0040901	4.52986	0.62025	2161.15	0.85669	1268.59	0.043031
60	0.67413	2.87011	0.0040960	4.25677	0.61380	2130.43	0.85235	1704.11	0.039385
61	0.71418	10.85293	0.0041149	5.89075	0.46834	2857.17	0.87550	3654.17	0.029955
62	0.71453	3.64072	0.0041782	4.87424	0.57861	1267.70	0.82211	3508.17	0.241737
63	0.59110	17.64547	0.0040992	6.58550	0.32734	3931.30	0.90754	5156.66	0.036278
64	0.70263	7.53089	0.0040814	4.93891	0.50679	2519.67	0.85818	3314.62	0.030514
65	0.68049	5.47418	0.0040829	4.89696	0.51113	2340.07	0.85296	2342.68	0.035662
66	0.68203	4.26608	0.0040667	4.50318	0.55257	2076.39	0.84151	1666.56	0.040801
67	0.68121	6.83128	0.0040486	4.39869	0.51675	2003.00	0.83437	1410.45	0.034780
68	0.68532	1.27070	0.0040553	4.62946	0.57428	1626.28	0.81858	995.68	0.055319
69	0.68715	5.75613	0.0040491	4.35700	0.52496	2207.32	0.83796	1579.51	0.027165
70	0.61884	14.12746	0.0040596	5.83039	0.37755	3645.89	0.87823	3411.77	0.016392
71	0.71801	6.69476	0.0040603	4.93612	0.47961	2719.03	0.85249	1885.84	0.019713
72	0.83048	3.06189	0.0040511	3.58030	0.59082	2346.10	0.83713	1221.99	0.020072
73	1.12200	10.81081	0.0033008	1.37671	0.76512	2003.73	0.82269	1110.57	0.024958
74	1.23810	2.71007	0.0040961	1.22895	0.98598	1232.39	0.79066	155.42	0.047294
75	1.04500	0.52345	0.0040244	1.40380	0.85510	1461.39	0.79677	503.34	0.036789
76	1.07330	0.46160	0.0040203	1.30141	0.87043	1473.54	0.79687	443.09	0.036301

Table 1. Coefficients for low-energy proton electronic stopping power parameterization. (continued)

Z_2	v_F	A_1	A_2	A_3	A_4	A_5	A_6	A_7	A_8
77	1.09530	0.97814	0.0040374	2.01267	0.72250	1890.81	0.81747	930.70	0.027690
78	1.23810	3.20857	0.0040510	3.66577	0.53618	3091.16	0.85602	1508.12	0.015401
79	1.28790	2.00351	0.0040431	7.48824	0.35610	4464.33	0.88836	3966.54	0.012839
80	0.78654	15.42995	0.0039432	1.12374	0.70703	4595.72	0.88437	1576.47	0.008853
81	0.66401	3.15124	0.0040524	4.09956	0.54250	3246.31	0.85772	1691.77	0.015058
82	0.84912	7.18963	0.0040588	8.69271	0.35842	4760.56	0.88833	2888.27	0.011029
83	0.88433	9.32087	0.0040540	11.54282	0.32027	4866.16	0.89124	3213.38	0.011935
84	0.80746	29.24222	0.0036195	0.16864	1.12264	5687.96	0.89812	1033.26	0.007130
85	0.43357	1.85222	0.0039973	3.15560	0.65096	3754.97	0.86383	1602.02	0.012042
86	0.41923	3.22200	0.0040041	5.90236	0.52678	4040.15	0.86804	1658.35	0.011747
87	0.43638	9.34124	0.0039661	7.92099	0.42977	5180.90	0.88773	2173.16	0.009201
88	0.51464	36.18267	0.0036003	0.58341	0.86747	6990.21	0.91082	1417.10	0.006219
89	0.73087	5.92839	0.0039695	6.40824	0.52122	4619.51	0.88083	2323.52	0.011627
90	0.81065	5.24536	0.0039744	6.79689	0.48542	4586.31	0.87794	2481.50	0.011282
91	1.95780	33.70174	0.0036901	0.47257	0.89235	5295.69	0.88930	2053.30	0.009191
92	1.02570	2.75890	0.0039806	3.20915	0.66122	2505.37	0.82863	2065.14	0.022816

Table 2. Coefficients for high-energy proton electronic stopping power parameterization.

Z_2	A_9	A_{10}	A_{11}	A_{12}	Z_2	A_9	A_{10}	A_{11}	A_{12}
1	4.17923×10^{-3}	1.85351×10^2	1.73395×10^2	1.03342×10^{-8}	47	1.52977×10^{-1}	5.52331×10^3	-1.31881×10^6	3.32296×10^{-7}
2	7.87969×10^{-3}	3.37897×10^2	-1.21551×10^4	1.92256×10^{-8}	48	1.55788×10^{-1}	5.66333×10^3	-1.42129×10^6	3.43645×10^{-7}
3	1.17242×10^{-2}	4.99690×10^2	-2.05489×10^4	2.84849×10^{-8}	49	1.58932×10^{-1}	5.74463×10^3	-1.43497×10^6	3.47382×10^{-7}
4	1.53771×10^{-2}	6.39460×10^2	-2.52185×10^4	3.62232×10^{-8}	50	1.60761×10^{-1}	5.80360×10^3	-1.55052×10^6	3.54295×10^{-7}
5	1.88005×10^{-2}	7.85353×10^2	-5.81862×10^4	4.55928×10^{-8}	51	1.64200×10^{-1}	5.97036×10^3	-1.61215×10^6	3.65844×10^{-7}
6	2.25672×10^{-2}	9.33404×10^2	-6.12123×10^4	5.37140×10^{-8}	52	1.68822×10^{-1}	6.05229×10^3	-1.47984×10^6	3.63253×10^{-7}
7	2.61772×10^{-2}	1.07594×10^3	-7.38496×10^4	6.19253×10^{-8}	53	1.73337×10^{-1}	6.25893×10^3	-1.47965×10^6	3.74553×10^{-7}
8	2.96061×10^{-2}	1.20559×10^3	-9.10080×10^4	6.95374×10^{-8}	54	1.76177×10^{-1}	6.36538×10^3	-1.53822×10^6	3.82146×10^{-7}
9	3.28578×10^{-2}	1.32120×10^3	-1.11202×10^5	7.64117×10^{-8}	55	1.76210×10^{-1}	6.47955×10^3	-1.87545×10^6	4.02778×10^{-7}
10	3.60771×10^{-2}	1.44270×10^3	-1.40758×10^5	8.40467×10^{-8}	56	1.81909×10^{-1}	6.52962×10^3	-1.62147×10^6	3.92193×10^{-7}
11	4.04266×10^{-2}	1.55387×10^3	-5.48654×10^4	8.58005×10^{-8}	57	1.83401×10^{-1}	6.66321×10^3	-1.84280×10^6	4.08537×10^{-7}
12	4.27369×10^{-2}	1.71185×10^3	-2.09978×10^5	1.01158×10^{-7}	58	1.88362×10^{-1}	6.67157×10^3	-1.61720×10^6	3.96734×10^{-7}
13	4.56765×10^{-2}	1.83950×10^3	-2.75340×10^5	1.10651×10^{-7}	59	1.90072×10^{-1}	6.80044×10^3	-1.81380×10^6	4.11707×10^{-7}
14	4.98400×10^{-2}	1.97154×10^3	-2.27594×10^5	1.15392×10^{-7}	60	1.93086×10^{-1}	6.85616×10^3	-1.81714×10^6	4.13253×10^{-7}
15	5.30531×10^{-2}	2.09546×10^3	-2.61762×10^5	1.23310×10^{-7}	61	1.97060×10^{-1}	6.95911×10^3	-1.77715×10^6	4.15753×10^{-7}
16	5.62856×10^{-2}	2.21626×10^3	-2.91405×10^5	1.30771×10^{-7}	62	1.99197×10^{-1}	7.07103×10^3	-1.91805×10^6	4.27100×10^{-7}
17	6.00254×10^{-2}	2.37308×10^3	-3.08937×10^5	1.40031×10^{-7}	63	2.03901×10^{-1}	7.13989×10^3	-1.77658×10^6	4.22819×10^{-7}
18	6.34885×10^{-2}	2.48602×10^3	-3.09324×10^5	1.45714×10^{-7}	64	2.06590×10^{-1}	7.20210×10^3	-1.81810×10^6	4.26463×10^{-7}
19	6.61386×10^{-2}	2.61892×10^3	-4.02448×10^5	1.57037×10^{-7}	65	2.08873×10^{-1}	7.30450×10^3	-1.92452×10^6	4.36101×10^{-7}
20	7.06403×10^{-2}	2.71378×10^3	-2.83540×10^5	1.56347×10^{-7}	66	2.11796×10^{-1}	7.42092×10^3	-1.98599×10^6	4.44400×10^{-7}
21	7.27608×10^{-2}	2.82763×10^3	-4.14705×10^5	1.67825×10^{-7}	67	2.14077×10^{-1}	7.44650×10^3	-2.01829×10^6	4.45809×10^{-7}
22	7.49584×10^{-2}	2.95813×10^3	-5.55519×10^5	1.80782×10^{-7}	68	2.17372×10^{-1}	7.64665×10^3	-2.12622×10^6	4.61611×10^{-7}
23	7.91888×10^{-2}	3.04568×10^3	-4.62426×10^5	1.80519×10^{-7}	69	2.19975×10^{-1}	7.62469×10^3	-2.08183×10^6	4.56486×10^{-7}
24	8.16522×10^{-2}	3.14779×10^3	-5.50701×10^5	1.89345×10^{-7}	70	2.23522×10^{-1}	7.69987×10^3	-2.04404×10^6	4.57783×10^{-7}
25	8.45124×10^{-2}	3.24460×10^3	-5.97089×10^5	1.95891×10^{-7}	71	2.25289×10^{-1}	7.78858×10^3	-2.18576×10^6	4.68159×10^{-7}
26	8.78728×10^{-2}	3.35075×10^3	-6.06019×10^5	2.01321×10^{-7}	72	2.27765×10^{-1}	7.89050×10^3	-2.27431×10^6	4.76889×10^{-7}
27	9.08265×10^{-2}	3.43834×10^3	-6.35674×10^5	2.06443×10^{-7}	73	2.31358×10^{-1}	7.92833×10^3	-2.19599×10^6	4.73988×10^{-7}
28	9.44268×10^{-2}	3.53336×10^3	-6.11897×10^5	2.09676×10^{-7}	74	2.28110×10^{-1}	8.16002×10^3	-2.94915×10^6	5.21279×10^{-7}
29	9.70308×10^{-2}	3.63804×10^3	-6.97379×10^5	2.18179×10^{-7}	75	2.35299×10^{-1}	8.10728×10^3	-2.44245×10^6	4.93146×10^{-7}
30	1.01064×10^{-1}	3.76368×10^3	-6.62649×10^5	2.22804×10^{-7}	76	2.38183×10^{-1}	8.18025×10^3	-2.49027×10^6	4.97212×10^{-7}
31	1.03813×10^{-1}	3.87169×10^3	-7.31501×10^5	2.31014×10^{-7}	77	2.41184×10^{-1}	8.23883×10^3	-2.48729×10^6	4.98990×10^{-7}
32	1.08558×10^{-1}	3.99456×10^3	-6.28264×10^5	2.32273×10^{-7}	78	2.44759×10^{-1}	8.28482×10^3	-2.41345×10^6	4.96956×10^{-7}
33	1.10147×10^{-1}	4.07755×10^3	-7.81829×10^5	2.42794×10^{-7}	79	2.48248×10^{-1}	8.43317×10^3	-2.47420×10^6	5.06469×10^{-7}
34	1.13619×10^{-1}	4.22875×10^3	-8.26686×10^5	2.52509×10^{-7}	80	2.50960×10^{-1}	8.47029×10^3	-2.46266×10^6	5.07107×10^{-7}
35	1.17630×10^{-1}	4.34695×10^3	-7.86689×10^5	2.56540×10^{-7}	81	2.53520×10^{-1}	8.59960×10^3	-2.55377×10^6	5.18382×10^{-7}
36	1.20336×10^{-1}	4.46509×10^3	-8.70085×10^5	2.65922×10^{-7}	82	2.57190×10^{-1}	8.70207×10^3	-2.51461×10^6	5.21905×10^{-7}
37	1.21919×10^{-1}	4.62546×10^3	-1.10030×10^6	2.84798×10^{-7}	83	2.60218×10^{-1}	8.80265×10^3	-2.55391×10^6	5.28151×10^{-7}
38	1.27026×10^{-1}	4.69242×10^3	-9.08710×10^5	2.78534×10^{-7}	84	2.62536×10^{-1}	8.92190×10^3	-2.65304×10^6	5.39186×10^{-7}
39	1.30043×10^{-1}	4.78771×10^3	-9.41457×10^5	2.84240×10^{-7}	85	2.65692×10^{-1}	9.03749×10^3	-2.69021×10^6	5.46553×10^{-7}
40	1.32588×10^{-1}	4.87865×10^3	-1.01440×10^6	2.91492×10^{-7}	86	2.71675×10^{-1}	9.15297×10^3	-2.62905×10^6	5.43040×10^{-7}
41	1.35950×10^{-1}	4.97111×10^3	-1.01510×10^6	2.95396×10^{-7}	87	2.74509×10^{-1}	9.16992×10^3	-2.58884×10^6	5.40957×10^{-7}
42	1.36106×10^{-1}	5.16807×10^3	-1.41996×10^6	$3.24194 \times 10^{-7}</$					

Proton stopping, $S_t(^1\text{H})$, in various target materials for $10 \text{ keV} \leq E \leq 100 \text{ MeV}$, calculated with TRIM² using the above parameterization, is plotted on the upper curves in Figure 3. High-energy proton stopping $S_e \approx S_t$, calculated using the parameterization in equation (9), for $10 \text{ MeV} \leq E \leq 2 \text{ GeV}$ is given on the lower curves in Figure 3. Proton stopping for $1 \text{ keV} \leq E \leq 10 \text{ GeV}$ and $Z_2 \leq 92$, based on a combination of theoretical calculations and experimental data (for $20 \text{ keV} \leq E \leq 1 \text{ MeV}$), have been tabulated by Janni⁴. These values agree within 10% with those plotted in Figure 3.

For ions heavier than protons, the electron stopping power in a given material can be calculated from the proton stopping power in the same material using the generalized scaling relation

$$S_e = \frac{S_e^{\text{ref}}(\gamma Z_1)^2}{(Z_1^{\text{ref}})^2}, \quad (10)$$

where S_e^{ref} and Z_1^{ref} are for a reference ion (${}^1\text{H}$) moving at the same velocity (same energy/nucleon) as the projectile for which S_e is to be calculated. Here, γZ_1 is the effective charge for the projectile of interest.

For ${}^4\text{He}$ ions, Ziegler et al.¹ parameterize γ as a function of $B = \ln(E/M_1)$ as follows:

$$\gamma^2 = 1 - \exp(-0.2865 - 0.1266B + 0.001429B^2 - 0.02402B^3 + 0.01135B^4 - 0.001475B^5)c^2, \quad (11)$$

where

$$c = 1 + (0.007 + 0.00005Z_2)\exp(-(7.6 - \ln \frac{E}{M_1}))^2 \quad (12)$$

corrects for the polarization of the target atoms by the projectile (the " Z_1^3 effect"). $S_e({}^4\text{He})$ is given by equation (10) for $E({}^4\text{He}) > 4 \text{ keV}$; otherwise it is proportional to the ion velocity. $S_t({}^4\text{He})$ can then be obtained from equations (1) and (2).

For ions with $Z_1 > 2$,

$$\gamma = q + 0.5(1-q)(v_0/v_F)^2 \ln[1 + (2\Lambda v_F/(a_0 v_0))^2]C, \quad (13)$$

where v_F is the Fermi velocity for the target material (which is included in Table 1), $v_0 (= e^2/\hbar)$ is the Bohr velocity, a_0 is the Bohr radius (0.529177 \AA), and q is the degree of ionization of the ion given by

$$q = 1 - \exp(0.803y_r^{0.3} - 1.3167y_r^{0.6} - 0.38157y_r - 0.008983y_r^2). \quad (14)$$

C is a correction factor incorporating the experimentally established Z_1^3 ; C is given by

$$C = 1 + \frac{1}{Z_1^2}(0.18 + 0.0015Z_2)\exp(-(7.6 - (\ln \frac{E}{M_1}))^2), \quad (15)$$

and Λ is the ion screening length defined in reference 1 as

$$\Lambda = \frac{2a_0(1-q)^{2/3}}{Z_1^{1/3}(1 - (1-q)/7)}. \quad (16)$$

The effective ion velocity, y_r , is given in terms of ion velocity v_1 ($\equiv \sqrt{2E/M_1}$). For $v_1 \geq v_F$,

$$y_r = \frac{v_1}{v_0 Z_1^{2/3}} \left(1 + \frac{v_F^2}{5v_1^2}\right), \quad (17)$$

and for $v_1 < v_F$,

$$y_r = \frac{0.75v_F}{v_0 Z_1^{2/3}} \left[1 + \left(\frac{2v_1^2}{3v_F^2}\right) - \frac{1}{15} \left(\frac{v_1}{v_F}\right)^4\right]. \quad (18)$$

These relations hold for ion velocities greater than $v_F/Z_1^{2/3}$; otherwise, S_e is proportional to velocity, except for $Z_2=6$ or for $Z_1 \leq 19$ in $Z_2=14$ or 32 band-gap materials, where it is proportional to $v_1^{0.75}$. An alternate parameterization based on $S({}^4\text{He})$ has been derived by Hubert et al.⁵. They tabulate stopping powers and ranges for ion beams with $2 \leq Z_1 \leq 103$ and $2.5 \leq E/M_1 \leq 500 \text{ MeV/nucleon}$ on various targets.

⁴ J.F. Janni, *At. Data Nucl. Data Tables* **27**, 147(1982).

⁵ F. Hubert, R. Bimbot, and H. Gauvin, *At. Data and Nucl. Data Tables* **46**, 1(1990).

Range: The pathlength for a projectile of energy E_0 in the stopping material is calculated from

$$R_t(E_0) = \int_0^{E_0} S_t^{-1} dE , \quad (19a)$$

which can also be expressed as

$$R_t(E_0) = R_t(E_1) + \int_{E_1}^{E_0} S_t^{-1} dE . \quad (19b)$$

However, the quantity which is most often measured is the projected (mean) range R_p , which is the mean distance travelled by the projectile in its incident direction. $R_p < R_t$ because of significant angular deflections of the projectile in collisions which become important when the energy is low enough for nuclear collisions to become significant. TRIM includes a Monte Carlo calculation which provides a full statistical accounting of the projectile's interaction with its stopping medium. Ziegler *et al.* also provide an algorithm for calculating R_p and its longitudinal and transverse standard deviations (range straggling) which provides calculational simplicity while giving satisfactory agreement with the full Monte Carlo calculations. To second order, it involves iterating the differential equation

$$R_p(E_0 + \Delta E_0) = R_p(E_0) + \left[\frac{4E^2 - 2E\mu S_n + \mu Q_n R_p(E_0)}{2(2ES_t - \mu Q_n)} \right] \frac{\Delta E_0}{E} . \quad (20)$$

Here, $\mu = \frac{M_1}{M_2}$, the initial value of R_p is calculated at $E_1 = 10$ eV/nucleon as

$$\frac{2E_1}{1.2S_t + \mu S_n} , \quad (21)$$

and Q_n is the second moment of the nuclear energy loss, given in units of $(\text{eV})^2/\text{\AA}$ by

$$Q_n = \frac{4M_1 M_2}{(M_1 + M_2)^2 (4 + 0.197\epsilon^{-1.691} + 6.684\epsilon^{-1.0494})} \frac{0.6022\rho}{M_2} \left(\frac{f_S}{f_\epsilon} \right) , \quad (22)$$

where ρ is the target material density (g/cm^3), f_S is the factor multiplying $S_n(\epsilon)$ in equation (2), and f_ϵ is the factor multiplying $(\frac{E}{M_1})$ in equation (3). With S_n and S_t in units of $\text{eV}/\text{\AA}$, equation (20) yields R_p in units of \AA .

The projected range for protons in various target materials, calculated with TRIM for $10 \text{ keV} \leq E \leq 100 \text{ MeV}$ and by integrating the higher energy inverse stopping power S_e using the parameterization of equation (9) for $100 \text{ MeV} \leq E \leq 2 \text{ GeV}$, is given in Figure 4. At the higher energies, the projected range and the pathlength are nearly identical, and the contribution of S_n is negligible.

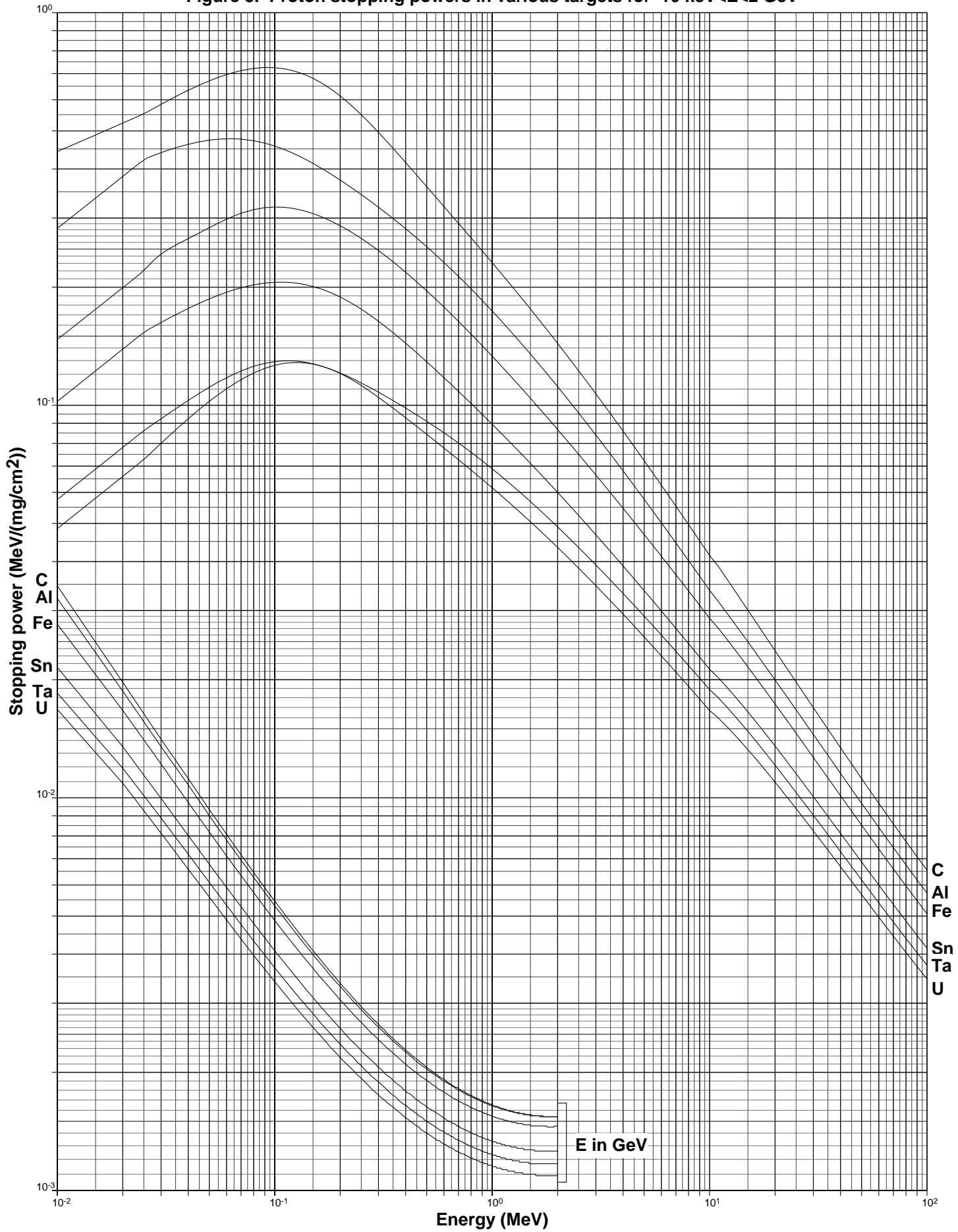
Figure 3. Proton stopping powers in various targets for $10 \text{ keV} < E < 2 \text{ GeV}$ 

Figure 4. Proton projected ranges in various targets for $10 \text{ keV} < E < 2 \text{ GeV}$ 